UNIVERSITY OF NIŠ
The scientific journal **FACTA UNIVERSITATIS**
Series: **Mechanics, Automatic Control and Robotics** Vol.2, No 7/2, 1997 pp. 353 - 368
Editor of series: Katica (Stevanovi}) Hedrih, e-mail: katica@masfak.masfak.ni.ac.yu
Address: Univerzitetski trg 2, 18000 Niš, YU, Tel: (018) 547-095, Fax: (018)-540-950
http:// ni.ac.yu/Facta

ON THE PROBLEM OF THE FLOW CONTROL BY BODY DEFORMABILITY

UDC: 532, 532.517.4

Samir Hanchi, Radomir Ašković

Abstract. *The development of a two-dimensional viscous incompressible flow generated from a deformable circular cylinder impulsively started into rectilinear motion is studied numerically for the Reynolds numbers equal to 550 and 1000. The vorticity transport equation is solved by a second-order finite-difference method in both directions of the domains. The Poisson equation for the stream function is solved by a Fourier-Galerkin method in the one direction of the flow which we assume to remain symmetrical and second-order finite-difference. The advances in time are second-order Adams-Bashforth. The computed results are compared qualitatively with experimental and numerical results done before in the particular nondeformable case. The comparison is found to be satisfactory.*

1. INTRODUCTION

Despite the simplicity of the obstacle geometry, the flow structure around an impulsively started circular cylinder (nondeformable) into rectilinear motion is complex, and all the phenomena of fluid mechanics are present. That is why, for more than a century, numerous theoretical, computational and experimental investigations of this problem have been reported in the literature.

Theoretical investigations of an impulsively started flow were frst undertaken by Blasius in 1908 [2], who obtained the first two terms of a time series solution of the boundary layer equations. Subsequently there have been many works attempting to obtain higher-order terms and advance the solution beyond the separation stage. Goldstein and Rosenhead [9], Schuh [20], Wundt [30] and Watson [29] have all considered this problem in the limiting case of infinite Reynolds number. Some authors (Wang [27], Collins and Dennis [6] [7], Bar-Lev and Yang [1] and Jovanovic et al. [13]) have extended their works to finite and high Reynolds numbers. In Collins and Dennis the problem is formulated in boundary layer variables and an expansion in powers of time is obtained. These expansions are corrected to take into account finite Reynolds number effects and are adjusted to match the uniform flow far from the cylinder. In Bar-Lev and

Received September 14, 1997

Yang the vorticity equation is solved by the method of matched asymptotic expansions. Inner (rotational flow) and outer (potential flow) solutions are obtained to third order in time and a composite solution is formed. The last two works provide extensive information for flow quantities of interest (such as vorticity field, streamlines, body forces). In Jovanovic et al. the unsteady boundary layer equation of second order is solved by the parametric method of matched asymptotic expansions. All these works are valid for relatively short times and the range of validity increases with increasing Reynolds number.

The second class is that of purely numerical solutions of the Navier-Stokes equations. Chronologically, Thom [25] gave the first numerical solution of steady Navier-Stokes equations corresponding to viscous flow around a circular cylinder. Unsteady flow was first studied by Payne [19] for Reynolds numbers equal to 40 and 100. Kawaguti and Jain [14], Son and Hanratty [22], Jain and Rao [12], Thoman and Szewczyk [26], Dennis and Staniforth [32], Collins and Dennis [6] [7], Patel [17] and Daube and Ta Phuoc Loc [8] investigated this problem for different Reynolds numbers. The common points of interest of these papers are the development of the primary unsteady wake length behind the cylinder and the evolution in time of the drag coefficient and separation angle.

In all these references, the problem is formulated in vorticity-stream function variables, and then Eulerian, Lagrangian and hybrid methods have been used for their discretization. Numerous computations have been performed in the last 30 years on this flow, but there are still open questions as to whether the numerics inteirfere with the physics of the problem, especially for the high Reynolds number flows. Ta Phuoc Loc [23] uses a fourth-order scheme to resolve the Poisson equation for the stream function and a second-order finite difference scheme for the vorticity transport equation. He presented computations for a range of Re (550-l000) and detailed diagnostics and comparisons with experimental results. This work was extended to higher Re (3000-9500) by Ta Phuoc Loc and Bouard [24]. Lecointe and Piquet [16] tested several high-order compact finite-difference schemes as well and they presented accurate computations for Re up to 550 and tentative simulations for higher values of Re. A more recent work is that of Wang and Dalton [28]. They used a predictor-corrector finite-difference sclleme for the vorticity transport equation and a fast Puisson solver for the stream function. They presented results for impulsively started and stopped flows for Re of 102 and 550.

More recently, some new numerical procedures, called vortex methods, are used to integrate the vorticity-velocity formulation of the Navier-Stokes equations. In vortex methods the most notable studies are those of Smith and Stansby [21]. Chang and Chern [4] and Koumoutsakos and Leonard [15]. The first two investigations use the Cloud-in Cell method (Christiansen [5]) to convect the vortices but use different techniques to take account for viscous effects. Smith and Stansby use the method of random walks whereas Chang and Chern use a finite-difference scheme on the grid used by the Cloud-in Cell technique to resolve the diffusion operator. Both works take advantage of the stability properties of vortex methods to extend their computations to very high Reynolds numbers (up to 10^6 in Chang and Chern). However, it appears that the increase in Re simulated is not followed by an adequate increase in the resolution. Recently, Anderson and Reider [31], and Wu et al. [35] conducted simulations of this flow using finite-difference schemes. Their simulations demonstrated the computational difficulties of the problem since very large numbers of grid points were necessary, in both works, to advance the

solution up to $t = 3$ for Re=9500.

Koumoutsakos and Leonard (1995) develped high-resolution direct numerical simulations using a novel adaptive numerical scheme for the enforcement of the no-slip condition for the vorticity-velocity formation of the Navier-Stokes equations. Their results, compared with some representative experimental, theoretical and computational works, provide benchmark quality simulations for the early stages of the flow around an impulsively started cylinder. Moreover, they identify the underlying mechanisms of unsteady separation and describe the effect of these phenomena on the drag coefficient.

Experimental investigations on unsteady flows resulting from an impulsive acceleration of a nondeformable cylinder date back to time of Prandtl [18]. Some experimental visualizations were described by Honji and Taneda [11] and Taneda [34]. However, the most extensive experiments to date seem to be those presented by Bouard and Coutanceau [3] for a translating cylinder. They analysed in detail the topological structure (formation and development of secondary vortices) of the flow around a cylinder by using the instantaneous velocity field and streamlines.

The complex problem of unsteady viscous flow around a deformable body is of interest as well in nature as in the technical practice (self-adaptable surfaces, for instance). The relevant physical problem could be also a nonviscometric flow in contact with the wall. The present work is concerned with the analysis of the flow structure at early times of the impulsively started uniformly deforming circular cylinder. The Poisson equation for the stream function is solved by a Fourier-Galerkin method coupled with a finite-difference method of second order. The vorticity transport equation is solved by a second-order Adams-Bashforth procedure, similar to Hakizumwami [10].

2. BASIC EQUATIONS

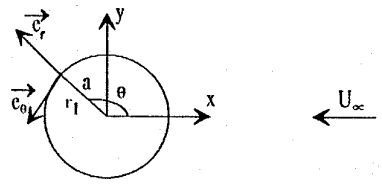

Figure l. System of coordinates

Let us consider the unsteady flow past a circular cylinder whose radius (of initial value a_0 grows uniformly with a constant factor of deformability A, started impulsively at the same time into rectilinear motion, with a constant velocity U_∞, in a $2D$ viscous incompressible fluid initially at rest. The unsteady Navier-Stokes equations in stream function and vorticity formulation for the flow past a circular cylinder can be written in polar coordinates as

$$\frac{\partial \overline{\omega}}{\partial t_1} = \frac{1}{r_1}\left[\frac{\partial}{\partial r_1}\left(\overline{\omega}\frac{\partial \psi_1}{\partial \theta}\right) - \frac{\partial}{\partial \theta}\left(\overline{\omega}\frac{\partial \psi_1}{\partial r_1}\right)\right] + \nu\nabla^2\overline{\omega}\,, \tag{1}$$

with $\overline{\omega} = \nabla^2\psi_1$ (2)

and $\nabla^2 = \frac{\partial^2}{\partial r_1^2} + \frac{1}{r_1}\frac{\partial}{\partial r_1} + \frac{1}{r_1^2}\frac{\partial^2}{\partial \theta^2}$,

where (r_1, θ) are polar coordinates (fig. 1), ν is the kinematic viscosity and t_1 is the time. The stream function ψ_1 is defined by

$$u_1 = -\frac{1}{r_1}\frac{\partial \psi_1}{\partial \theta} \quad \text{and} \quad v_1 = \frac{\partial \psi_1}{\partial r_1} \tag{3}$$

and the only nonzero component of the vorticity ϖ is

$$\varpi = \frac{1}{r_1}\left(\frac{\partial}{\partial r_1}(v_1 r_1) - \frac{\partial u_1}{\partial \theta}\right) \tag{4}$$

By introducing nondimensional quantities,

$$\frac{a}{a_0} = (1 + At)\,,\ r = \frac{r_1}{a} = e^{\xi}\,,\ R_e = \frac{2U_\infty a}{\nu}\,,\ t = \frac{t_1 U_\infty}{a_0}\,,\ \psi = \frac{\psi_1}{U_\infty a}\,,\ \omega = \frac{\varpi a}{U_\infty}\,, \tag{5}$$

(1) and (2) become

$$\frac{\partial \omega}{\partial t} = \frac{\omega}{a}\frac{\partial a}{\partial t} + \frac{a_0}{a}e^{-2\xi}\left[\frac{\partial \omega}{\partial \xi}\frac{\partial \psi}{\partial \theta} - \frac{\partial \omega}{\partial \theta}\frac{\partial \psi}{\partial \xi} + \frac{2}{R_e}\left(\frac{\partial^2 \omega}{\partial \xi^2} + \frac{\partial^2 \omega}{\partial \theta^2}\right)\right], \tag{6}$$

$$\nabla^2 \psi = e^{2\xi}\omega \tag{7}$$

where $\nabla^2 \psi = \frac{\partial^2 \psi}{\partial \xi^2} + \frac{\partial^2 \psi}{\partial \theta^2}$.

Initial conditions

The cylinder being suddenly started from the rest, has the following initial conditions:

$$\psi = 0 \ \text{and} \ \omega = 0 \quad \text{at} \quad t = 0 \tag{8}$$

Boundary conditions

***For** $\xi \to 0$

The cylinder being deformable, has velocity components at the wall of

$$u_1 = \frac{\partial a}{\partial t_1} \quad \text{and} \quad v_1 = 0$$

i.e., taking into account (4),

$$v_1 = \frac{\partial \psi_1}{\partial r_1} = 0 \quad \Rightarrow \quad \psi_1 \text{ is independent of } r_1\,,$$

$$u_1 = -\frac{1}{r_1}\frac{\partial \psi_1}{\partial \theta} = \frac{\partial a}{\partial t_1} \quad \text{whence} \quad \psi = -\frac{\theta}{a_0}\frac{\partial a}{\partial t}$$

It results from previous equation that ψ is a non uniform function on the surface of the cylinder. Hence, a uniform function is introduced as

$$\psi_u = \psi + \frac{\theta}{a_0}\frac{\partial a}{\partial t} \tag{9}$$

we can eliminate the stream function multiformity.

***For** $\xi \to \infty$

The stream-function of the flow past a deformable circular cylinder is well-known

$$\psi = 2\sinh(\xi_\infty)\sin(\theta) - \frac{\theta}{a_0 e^{\xi_\infty}}\frac{\partial a}{\partial t}$$

By introducing the uniform stream-function, the boundary condition is determined by (10),

$$\psi_u = 2\sinh(\xi_\infty)\sin(\theta) - \frac{\theta}{a_0 e^{\xi_\infty}}\frac{\partial a}{\partial t} + \frac{\theta}{a_0 e^{\xi_\infty}}\frac{\partial a}{\partial t} \tag{10}$$

For the downstream boundary condition at infinity an open boundary condition is established by assuming that the viscous-diffusive effect is negligible; then the vorticity equation will be,

$$\frac{\partial \omega}{\partial t} = \frac{\omega}{a}\frac{\partial a}{\partial t} + \frac{a_0}{a}e^{-2\xi}\left[\frac{\partial \omega}{\partial \xi}\left(\frac{\partial \psi_u}{\partial \theta} - \frac{1}{a_0}\frac{\partial a}{\partial t}\right) - \frac{\partial \omega}{\partial \theta}\frac{\partial \psi}{\partial \xi}\right] \tag{11}$$

$$\frac{\partial \psi}{\partial \theta} = \frac{1}{2\Delta\theta}(\psi_u(\xi_\infty, \theta + \Delta\theta) - \psi_u(\xi_\infty, \theta + \Delta\theta)) - \left(\frac{1}{a_0}\frac{\partial a}{\partial t}\right),$$

$$\frac{\partial \omega}{\partial \theta} = \frac{1}{2\Delta\theta}(\omega(\xi_\infty, \theta + \Delta\theta) - \omega(\xi_\infty, \theta - \Delta\theta))$$

$$\frac{\partial \psi}{\partial \xi} = \frac{1}{\Delta\xi}(\psi_u(\xi_\infty, \theta) - \psi_u(\xi_\infty - \Delta\xi, \theta)),$$

$$\frac{\partial \omega}{\partial \xi} = \frac{1}{\Delta\xi}\left(\frac{\omega^{n+1}(\xi_\infty, \theta) + \omega^{n-1}(\xi_\infty, \theta)}{2} - \omega(\xi_\infty - \Delta\xi, \theta)\right).$$

This condition is similar to the so-called “radiant Sommerfeld condition” [24].

The new system to resolve

The new system to resolve is determinated by (12) and (13),

$$\frac{\partial \omega}{\partial t} = \frac{\omega}{a}\frac{\partial a}{\partial t} + \frac{a_0}{a}e^{-2\xi}\left[\frac{\partial \omega}{\partial \xi}\left(\frac{\partial \psi_u}{\partial \theta} - \frac{1}{a_0}\frac{\partial a}{\partial t}\right) - \frac{\partial \omega}{\partial \theta}\frac{\partial \psi_u}{\partial \xi} + \frac{2}{R_e}\left(\frac{\partial^2 \omega}{\partial \xi^2} + \frac{\partial^2 \omega}{\partial \theta^2}\right)\right] \tag{12}$$

$$\Delta^2 \psi_u = e^{2\xi}\omega \tag{13}$$

with the new boundary conditions,

$$\psi_u = 0 \qquad \text{for} \qquad \xi = 0$$

$$\left.\begin{aligned}\psi_u &= 2\sinh(\xi_\infty)\sin(\theta) - \frac{\theta}{a_0 e^{\xi_\infty}}\frac{\partial a}{\partial t} + \frac{\theta}{a_0 e^{\xi_\infty}}\frac{\partial a}{\partial t} \\ \frac{\partial \omega}{\partial t} &= \frac{\omega}{a}\frac{\partial a}{\partial t} + \frac{a_0}{a}e^{-2\xi}\left[\frac{\partial \omega}{\partial \xi}\left(\frac{\partial \psi_u}{\partial \theta} - \frac{1}{a_0}\frac{\partial a}{\partial t}\right) - \frac{\partial \omega}{\partial \theta}\frac{\partial \psi}{\partial \xi}\right]\end{aligned}\right\} \quad \text{for} \quad \xi \to \infty$$

3. BODY FORCES

The drag force may be computed as the sum of the pressure drag F_p and the friction drag F_f. The pressure drag can be determined from the vorticity flux on the cylinder surface as

$$\vec{F}_p = -\int_0^{2\pi}\left(\frac{2}{R_e}\frac{\partial \omega}{\partial \xi} + \frac{\partial \psi}{\partial \theta}\omega\right)\vec{e}_\theta d\theta \,, \tag{14}$$

while the friction drag may be computed from the vorticity on the cylinder surface as

$$\vec{F}_f = \int_0^{2\pi}\left(\frac{2\omega}{R_e}\right)\vec{e}_\theta d\theta \,. \tag{15}$$

Hence, the total drag force on the body follows

$$\vec{F}_T = \vec{F}_p + \vec{F}_f \,, \tag{16}$$

and the drag coefficient of the body is given by

$$C_D = \frac{\vec{F}_T \bullet \vec{e}_x}{U_\infty^2 a} \,. \tag{17}$$

4. NUMERICAL METHOD

The vorticity transport equation (6) can be written as

$$\frac{\partial \omega}{\partial t} = \frac{\omega}{a}\frac{\partial a}{\partial t} + \frac{a_0}{a}e^{-2\xi}G \tag{18}$$

where

$$G = \left[\frac{\partial \omega}{\partial \xi}\left(\frac{\partial \psi_u}{\partial \theta} - \frac{1}{a_0}\frac{\partial a}{\partial t}\right) - \frac{\partial \omega}{\partial \theta}\frac{\partial \psi_u}{\partial \xi} + \frac{2}{R_e}\left(\frac{\partial^2 \omega}{\partial \xi^2} + \frac{\partial^2 \omega}{\partial \theta^2}\right)\right]. \tag{19}$$

The second-order Adams-Bashforth temporal scheme is used together with central differences in space for equation (18) on a grid defined by $\xi_i = (i\text{-}1)\Delta\xi$, $i = 1,2,...,M$; $\theta_j = (j\text{-}1)\Delta\theta$, $j = 1,2,...,N$; $\Delta\xi = \xi_\infty / (M\text{-}1)$, and $\Delta\theta = \pi / (N\text{-}1)$. The domain is truncated in the ξ-direction at ξ_∞. As a result,

$$\omega_{i,j}^{n+1} = \omega_{i,j}^{n}\left[\frac{(1+At)}{(1+At)}\right] + \frac{\Delta t}{2}\left(\frac{1}{(1+At)}\right)e^{-2\xi}(3G_{i,j}^{n} - G_{i,j}^{n-1})$$

and

$$G_{i,j} = \frac{\psi_{ui,j+1} - \psi_{ui,j-1}}{2\Delta\theta}\frac{\omega_{i+1,j} - \omega_{i-1,j}}{2\Delta\xi} - \frac{\psi_{ui+1,j} - \psi_{ui-1,j}}{2\Delta\xi}\frac{\omega_{i,j+1} - \omega_{i,j-1}}{2\Delta\theta} +$$
$$+ \frac{2}{R_e}\left(\frac{\omega_{i-1,j} - 2\omega_{i,j} + \omega_{i+1,j}}{(\Delta\xi)^2} + \frac{\omega_{i,j-1} - 2\omega_{i,j} + \omega_{i,j+1}}{(\Delta\theta)^2}\right)$$

By using the following expansions for ψ_u and ω:

$$\psi_u(\xi,\theta,t) = \sum_{n=1}^{N} f_n(\xi,t)\sin(n\theta)\,, \tag{20}$$

$$\omega(\xi,\theta,t) = \sum_{n=1}^{N} F_n(\xi,t)\sin(n\theta)\,, \tag{20}$$

the equation (7) becomes

$$\int_0^{\pi}\left(\frac{\partial^2\psi_u}{\partial\xi^2} + \frac{\partial^2\psi_u}{\partial\theta^2}\right)\sin(m\theta)d\theta = \int_0^{\pi} e^{2\xi}\sin(m\theta)d\theta\,.$$

Orthogonality of the basis and trial functions implies

$$\frac{\partial^2 f_n}{\partial\xi^2} - n^2 f_n = e^{2\xi}F_n\,, \tag{22}$$

which defines a system of equations in Fourier space, with the next boundary conditions,

$$f_n(0,t) = 0 \qquad \text{and} \qquad f_n(\xi_\infty,t) = \frac{2}{\pi}\int_0^{\pi}\psi_u(\xi_\infty,\theta,t)\sin(n\theta)$$

Equation (22) is discretized in the Fourier space using central differences so that

$$f_{n,i-1} - |\,2 + (\Delta\xi)^2 n^2\,|\,f_{n,i} + f_{n,i+1} = (\Delta\xi)^2 e^{2\xi}F_{n,i} \tag{23}$$

Equations (23) defines a tridiagonal system of equations. An inverse Fourier transform on the solution of (23) yields the corresponding solution in physical space (ψ_{ij}).

It remains only to determine the surface vorticity over the cylinder (equivalently the boundary condition for equation (18)).

Equation (7) at $\xi = 0$ is

$$\frac{\partial^2\psi}{\partial\xi^2} = \omega(0,\theta,t) \tag{24}$$

A Taylor expansion yields a second-order equation for $\omega(0,\theta,t)$,

$$\omega_{1,j} = \frac{1}{2(\Delta\xi^2)}(-7\psi_{1,j} + 8\psi_{2,j} - \psi_{3,j}) \tag{25}$$

So, similar to [10], the seqence of the numerical calculations is the following:

1 - Initially, we consider an irrotational flow, $\omega(0,\theta,t)$-0.
2 - Fourier sine transform ω. Fourier sine transform boundary condition at infinity. Solve the Poisson equation for the stream-function in the Fourier space. Take the inverse Fourier sine transform of the solution.
3 - The solution in the previous step is used to update the vorticity along of the cylinder surface to satisfy the no-slip condition.
4 - Construct new values for the vorticity by solving the transport equation, with appropriate time marching.
5 - Repeat all steps from the step 2.

5. RESULTS

First of all, if a circular cylinder was deformed (with a radius growing or reducing in time) in a fluid at rest, the flow streamlines would be rectilinear as it is shown by the following sketch.

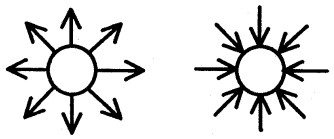

Growing radius Reducing radius

Now, we will study the flow structure around an impulsively started and uniformly deforming circular cylinder for differeent Reynolds numbers at early time.

For the numerical calculations, for all Reynolds numbers: the time step is $\Delta t = 0.01$, the grid size is 90×180 and ξ_∞ is equal to 1.6094.

5.1 $Re_0 = 550$

5.1.1 The flow structure

a) Nondeformable cylinder

The flow structure past an impulsively started nondeforming circular cylinder is complex. The streamline history of the flow field is presented in Figure 2. Beside the primary vortex, the appearance of a small secondary region can be observed. The streamline patterns show the appearance of a secondary vortex at $t = 3$ (Fig. 2). The secondary vorticity is also visible in the vorticity plots at $t = 2$. The secondary vorticity remains confined after its initial appearance. Its evolution is mainly affected by the dynamics of the primary vortex. As the secondary vortex grows it penetrates the primary vortex, but it is never able to reach the outer irrotational flow field. It seems that a stable configuration (the so-called α-phenomenon) is established before $t = 4$.

The interplay of primary and secondary vorticity is manifested in the drag curve. After its initial drop, the appearance and growth of the secondary vortex increases the drag coefficient as the primary vortex is pushed outwards. This increase reaches a maximum at $t = 3$ (fig. 3) beyond which the strength and the size of the secondary vortex are reduced whereas the primary vortex is further convected by the free stream velocity.

The drag decays to its steady state value while symmetry persists.

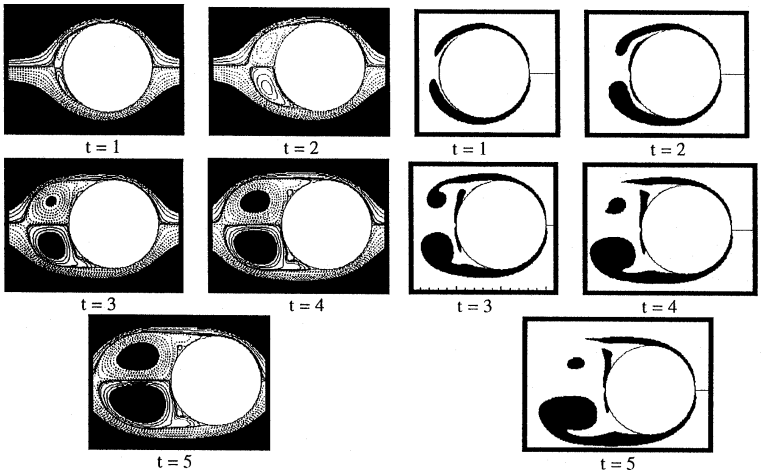

Instantaneous streamlines Equi-vorticity contour

Figure 2. Evolution of the flow structure for Re0 = 550 and A=0

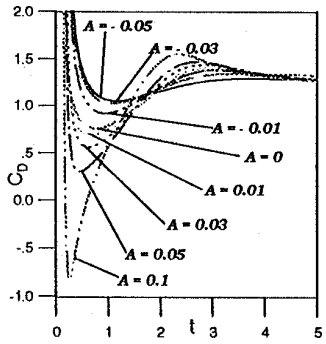

Figure 3. Drag coefficient of an impulsively started deformable cylinder at Re = 550

Finally, we may observe the similarity of our results with these previously obtained numerically by Koumoutsakos and Leonard and experimentally by Bouard and Coutanceau.

b) Deforming circular cylinder: $a = a_0 (1 + At)$

Case of the growing radius (A > 0)

The impulsively setting of a growing circular cylinder in a rectilinear translation causes a backward deviation of streamlines issued from the body surface. This defiation causes some new phenomena beside those already announced before in the nondeformable case. As a matter of fact, the, the growing radius pushes the primary vortex away from the cylinder surface, renders the secondary vortex much stronger and it will be able to push the primary vortex away from the cylinder. However, it can not reach

the outer irrotationnal flow field. We can also see that the so-called α-phenomenon is established before $t = 3$ (fig. 4).

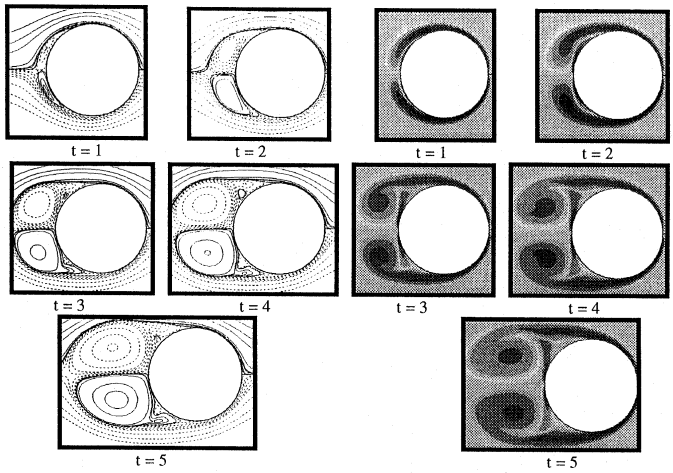

Instantaneous streamlines Equi-vorticity contour

Figure 4. Evolution of the flow structure for $Re_0 = 550$ and A = 0.015

Case of the reducing radius (A < 0)

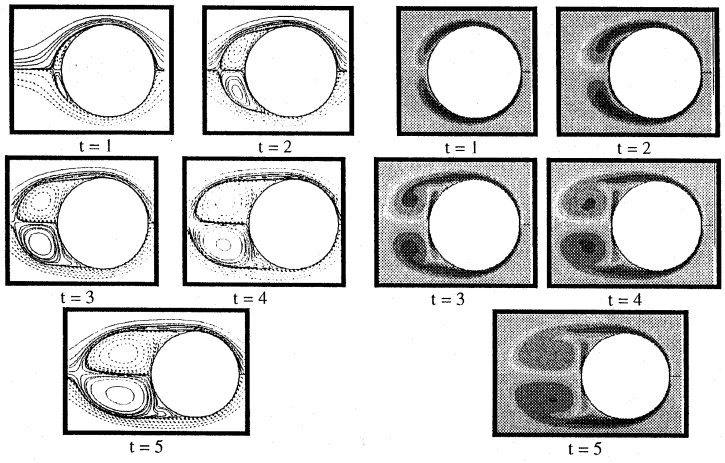

Instantaneous streamlines Equi-vorticity contour

Figure 5. Evolution of the flow structure for $Re_0 = 550$ and A = -0.015

In the case of a reducing radius, there is another new flow phenomenon behind the cylinder. In figure 5 the development of the flow structure is given. The cylinder with a reducing radius has tendency to attract the fluid towards its surface. So, the primary vortex is aspired by the cylinder and the formation of the secondary vortex is prevented.

5.1.2 Influence of body deformability on the drag coefficient

The following was discovered relative to the drag coefficient for a growing radius. Before the primary vortex formation, the fluid pushed outwards by the cylinder created a reaction force opposite to the drag force, in addition to the effects due to sudden translation. Therefore, the bigger deformability factor A, the stronger the reaction force and the force ratio becomes sufficient to overpower the drag force and to propel the deforming cylinder down flow in the cases A=0.1 for Re_0=5.50. However, the formation of primary vortex reduces the preceding effect. The primary and secondary developments increase both the wake behind the cylinder and the drag force as its consequence (fig. 3).

For a reducing radius, we can see that the attraction of the primary vortex by the cylinder and the absence of the secondary vortex reduce the wake behind the cylinder. As a consequence of this phenomenon, we observe on the drag curves (fig. 3) that the drag coefficient after its initial drop grows less rapidly than in the case of the nondeforming cylinder.

5.1.3 Influence of body deformability on the boundary layer separation

The curves of vorticity on the surface of the body show the following: the augmentation of the radius advances the boundary layer separation (fig. 6), similar to the wall-injection effect, while the reduction of the radius delays the boundary layer separation (fig. 6) as in the case of the wall-suction control.

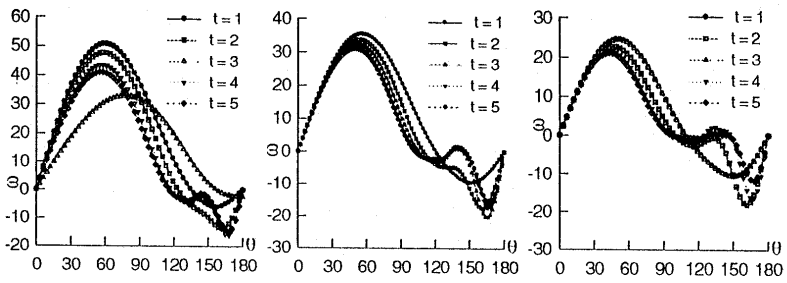

Figure 6. Vorticity on the surface of the body for Re=550

5.2 RE_0 = 1000

5.2.l The flow structure

a) Nondeformable cylinder

The time history of the flow structure for Re=1000 is shown in figure 7. Phenomena similar to those observed in the previous case Re=550 are present here as well. The primary vortex is formed at the rear of the cylinder and the secondary vortex, although stronger in this case remains confined by the primary vortex. The secondary vortex attempts to reach the outer flow field but stays blocked by the primary one.

All our results are similar to these previously obtained by Koumoutsakos and Lenoard and Bar-Lev and Yang, while large discrepancies appear between the results of the present study and those presented by Loc because of the different initial conditions.

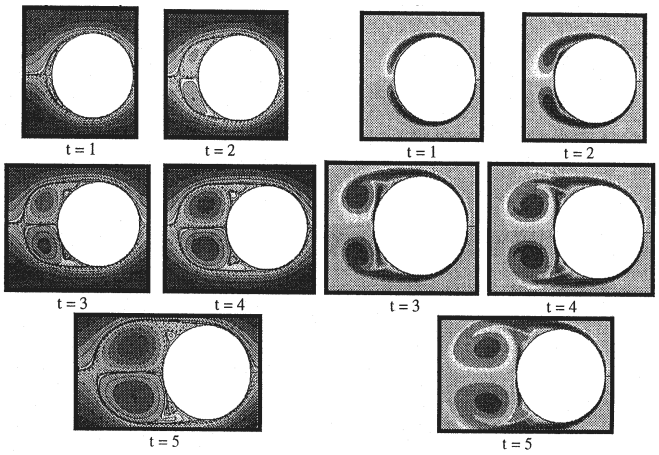

Instantaneous streamlines Equi-vorticity contour

Figure 7. Evolution of the flow structure for Re_0=1000 and A=0

b) Deforming circular cylinder: $a = a_0(1+At)$, (A>0 and A<0)

Also, all the phenomena similar to these observed in the previous case Re = 550 are present here, but in the more pronounced form. In fact, the augmentation of the radius implies that the secondary vortex becomes stronger than in the preceding Reynolds number case. This phenomena allows the secondary vortex to reach out the external irrotationnal flow for a deformability factor equal to 0.05 (fig. 10). The formation of the α-phenomenon takes place approximately at the same locations but at inferior times as in the analogous nondeformable case (fig. 8).

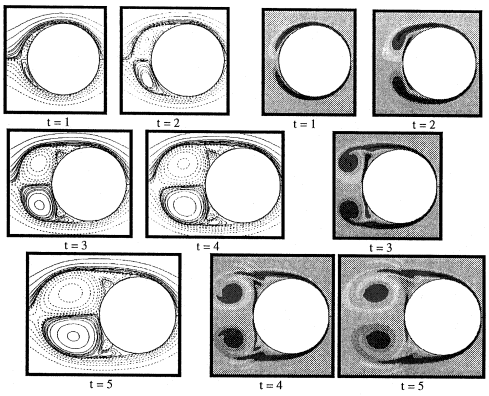

Instantaneous streamlines Edui-vorticity contour

Figure 8. Evolution of the flow structure for Re_0=1000 and A=0.015

As in the previous case (Re=550). the diminution of the radius of the circular cylinder prevents the formation of the secondary vortex and attracts the primary vortex towards the cylinder.

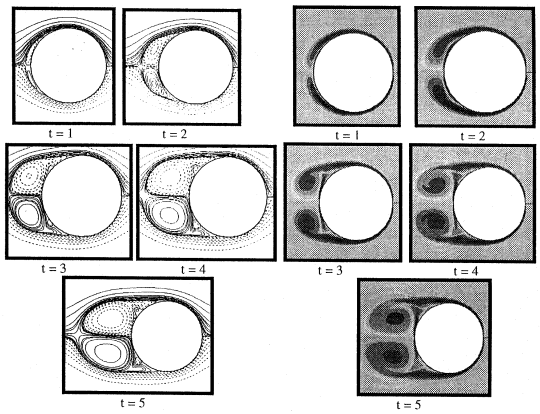

Instantaneous streamlines Equi-vorticity contnur

Figure 9. Evolution of the flow structure for Re_0 =1000 and A = -0.01.5

5.2.2 Influence of body deformability on the drag coefficient

Briefly, we may observe at Re=1000, for either a nondeformable or deformable circular cylinder, the same effects as those already observed in the previous case of Re=550. The only difference consists in a value of the deformability factor A (0.05 instead of 0.1) causing a propulsion of the cylinder (fig.10) in the case of the growing radius of a cylinder.

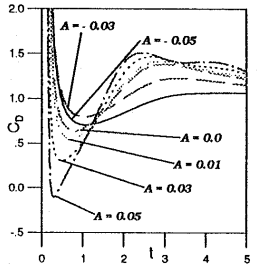

Figure 10. Drag coefficient of an impulsively started deformable cylinder at Re=1000

5.2.3 Influence of body deformability on the boundary layer separation

As the curves of vorticity on the surface of the body show again, the increase of the radius of the cylinder advances the boundary layer separation (fig. 11), having the same effect as wall-injection, while the decreasing of the radius delays the point of the boundary layer separation (fig. 11) similar to the classical wall-suction.

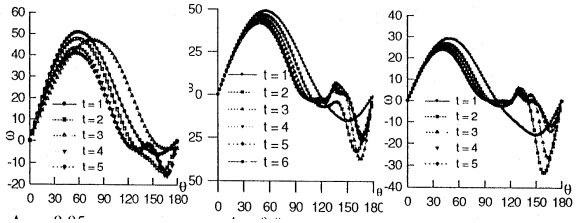

Figure 11. Vorticity on the surface of the body for Re=1000

6. CONCLUSIONS

The present numerical simulation is concerned with the analysis of unsteady separated flow at early times around the impulsively started uniformly deforming circular cylinder for two Reynolds numbers. Firstly, all the results including α-phenomenon, previously detected either numerically or by experimental visualisation, have been reproduced in detail in the preliminary nondeformable case. Then we have studied the interaction between vortical structures and deformable walls and their effect on the drag force experienced by the body. The interplay of these primary and secondary vorticies, on the one hand, and the deforming surface of the cylinder, on the other hand, is the underlying mechanism for drag reduction and increase. In fact, it has been shown here that, in both the cases of the growing radius of the cylinder and the reducing radius of the cylinder, the body deformability factor has a favorable effect on the drag coefficient, but for different physicals reasons. In fact, in the case of a growing radius the favorable effect comes from the force propulsion created by the body, and in the case of a reducing radius the favorable effect comes from the attraction of the primary vortex towards the cylinder. So, the body deformability may be used as a wake control device that would favorably effect the interplay of primary and seccondary vorticity, thus reducing the drag coefficient. Finally, we continue the numerical study of the flow at the greater Reynolds numbers as well as the heat transfer on a uniformly deforming cylinder, parallely using boundary layer approximation with some initial rather satisfactory results [33].

REFERENCES

1. Bar-Lev, M. and Yang, H. T., (1975), *Initial flow field over an impulsively started circular cylinder*, J. Fluid Mech., vol. 72, pp. 625-647.
2. Blasius, N., (1908), *Grenzchichten in Flussigkeiten mit Kleiner Reiburg*, Z. Angew, Math. Phys., NACA TM-1256 56, pp. 1.. (Engl. trans.)
3. Bouard, R. and Coutanceau, M., (l980), *The early stage of development of the wake behind an impulsively started cylinder for 40<Re<104*, J. Fluid Mech., vol. 233, pp. 243-263.
4. Chang, C. C. and Chern, R. L., (1991) *A numerical study of flow around an impulsively started circular cylinder by a deterministic vortex method*, J. Fluid Mech., vol. 233, pp. 243-263.
5. Christiansen, J. P., (1973) *Vortex methods for flow simulation*, J. Comput. Phys., vol. 13. pp, 363.
6. Collins, W. M. and Dennis, S. C. R, (1973a), *The initial flow past an impulsively started circular cylinder*, Q. J. Mech. Appl. Maths, vol. 26, pp. 53.
7. Collins, W. M. and Dennis, S. C. R., (1973b), *Flow past an impulsively started circular cylinder*, J. Fluid Mech., vol. 60, pp. 105.
8. Daube, O. and Ta Phouc Loc, (1978) *Etude numerique d'écoulements instationnaires de fluide visqueux incompressible autour de corps profilé par une methode combinée d'ordre 0(h2), 0(h4)*, J. Mec.,vol.17, pp. 651.
9. Goldstein, S. and Rosenhead, L., (1936), *Boundary layer growth*, Proc. Camb. Phil. Soc., vol. 32, pp. 392.
10. Hakizumwami, B. K., (1994), *High Reynolds number flow past an impulsively started circular cylinder*, Computers Fluids, vol. 7, pp. 895.
11. Honji, H: and Taneda, S., (1969), *Unsteady flow past a circular cylinder*, J. Phys. Soc. Japan vol. 27, pp. 1968.
12. Jain, P. C. and Rao, K. S., (1969) *Numerical solution of unsteady voscous incompressible fluid flow past a circular cylinder*, Phys. Fluids Suppl., vol. 12, pp. II-57.
13. Jovanovic, J. and Askovic, R. and Djuric, R., (l979), *Approximations superieures dans la theorie de la couche limite instationnaire et leur traitment parametrique*, GAMM-Tagung 1978, Brussels, ZAMM 59, pp. 240-243.

14. Kawaguti, M. and Jain, P.C., (l966) *Numerical study of a viscous fluid past a circular cylinder*, J. Phys. Soc. Japan, vol. 21, pp. 2055.
15. Koumoutsakos, P. and Leonard, A., (1995) *High-resolution simulations of the flow around and impulsively started cylinder using vortex method*, J. Fluid Mech., vol. 296, pp. 1-38.
16. Lecointe, Y. and Piquet, J., (1984) *On the use of several compact methods for the study of the incompressible viscous flow around a circular cylinder*, Comp. and Fluids, vol. 12, pp. 255-280.
17. Patel, V. A., (1976), *Time dependent solution of viscous incompressible flow a circular cylinder*, Comp. and Fluids, vol. 4, pp. 13.
18. Prandtl, W., (1925), *The magnus effect and wind powered ships*, Wissenschaften, vol. 13, pp. 93-108.
19. Payne, R. B., (1958), *Calculations of unsteady viscous flow past a circular cylinder*, J. Fluid Mech., vol. 4, pp. 81.
20. Schuh, H., (1953), *Calculation of unsteady boundary layers in two dimensinoal lalminar flow*, Z. Flugwiss., vol. 1, pp.122.
21. Smith, P. A. and Stansby, P. K., (1988), *Impulsively started flow arnund a circylar cylinder by the vortex method*, J. Fluid Mech., vol. 194, pp. 45-77.
22. Son, J. S. and Hanratty, T. J., (l969), *Numerical solution of the flow arnund a cylinder at Reynolds number of 40, 200, 500*, J. Fluid Mech., vol. 35, pp. 369.
23. Ta Phuoc Loc, (1980), *Numerical analysis of unsteady secondary vortices generated by an impulsively started circylar cylinder*, J. Fluid Mech., vol.100, pp. 111.
24. Ta Phuoc Loc and bouard, R., (1985), *Numerical solution of the early stage of the unsteady viscous flow around a circular cylinder: a comparison with experimental visualisation and measurements*, J. Fluid Mech., vol. 160, pp. 93.
25. Thom, A., (1933), *The flow past circular cylinders at low speeds*, Proc. R. Soc. Lond., A 141. pp. 651.
26. Thoman, D. C. and Szewczyk, A. A., (1969), *Time dependent viscous flow over a circular cylinder*, Phys Fluids, Suppl. 12, pp. II-76.
27. Wang, C. Y., (1967), *The flow past a circular cylinder which is started impulsively from rest*., J. Maths and Phys., vol. 46, pp. 195.
28. Wang, X. and Dalton, C., (1991), *Numerical solutions for impulsively started and decelerated viscous flow past a circular cylinder*, Intl J. Numer. Meth Fluids, vol. 12, pp. 383-400.
29. Watson, E. J., (1955), *Boundary layer growth*, Proc. R. Soc. London, A 231, pp. 104.
30. Wundt, H., (1955), *Wachstum der laminaren grenzschicht an schrag angestromten Zelindern bei Anfahrt aus der Ruhe*, Ing. – Arch. Berlin, vol. 23, pp. 212.
31. Anderson, C. R. and Reider, M., (1993), *Investigation of the use of Prandtl/Navier-Stockes equation procedures for two-dimensional incompressible flows*, CAM Rep. 93-02 Department of Mathematics, UCLA.
32. Dennis, S. C. R. and Staniforth, A. N., (1971), *A numerical method for calculating the initial flow past a cylinder in a viscous fluid*, In Proc., 2nd Intl Conf. on Numerical Methods in Fluid Dynamics (ed M. Holt), Lecture Notes in Physics, vol. 8, pp. 343, Springer.
33. Hanchi, S. and Askovic, R., (1995), *A method of parametric approximations for laminar MHD thermal boundary layer around a deformable body*, MAHYD 95, l4th International Riga Conference on Magneto hydrondynamics, 24-26 August 1995, Latvia.
34. Taneda, S., (1972), *Visualisation expelriments on unsteady viscous flows around cylinders and plates*, In Recent Research on Unsteady Boundary Layers, vol. 2, (ed. E. A. Eichelbrenner). Quebec Laval University.
35. Wu, J. Z. and Wu, X. and Ma, H. and Wu, J. M.б (1995) *Dynamic vorticity condition: theory and numerical implementation*. Intl J. Numer. Fluids (Submitted).

O PROBLEMU UPRAVLJANJA STRUJANJEM NA OSNOVU DEFORMABILNOSTI TELA

Samir Hanchi, Radomir Askovic

Razvoj dvodimenzionalnog viskoznog strujanja nestišljivog fluida nastalog usled kretanja deformabilnog kružnog cilindra koji impulsivno kreće u pravolinijsko kretanje se proučava

numerički za Rejnoldsove brojeve od 550 i 1000. Jednačina transporta vrtložnosti je rešena metodom konačnih razlika drugog reda u oba pravca posmatrane oblasti. Poisson-ova jednačina za strujnu funkciju je rešena pomoću Fourier-Galerkin metoda u jednom pravcu strujanja, za koji se pretpostavlja da konačne razlike ostaju simetrične i drugog reda. Vremenski pomeraji su drugog reda Adams-Boshforth-a. Proračunati rezultati se upoređuju kvalitativno sa eksperimentalnim i numeričkim rezultatima koji su dobijeni ranije za slučaj nedeformabilnog tela. Poređenja koja su izvršena su sasvim zadovoljavajuća.